RESEARCH ARTICLE

Embracing Small Satellites Into Future 6G Inclusive IoT Coverage: A Deployment of Diversity-Based Theoretical Framework

HAIDAR N. AL-ANBAGI[1,2], **(Member, IEEE), AND IVO VERTAT**[1]

[1]Department of Electronics and Information Technology, Faculty of Electrical Engineering, University of West Bohemia, 30100 Pilsen, Czech Republic
[2]Department of Communications Engineering, College of Engineering, University of Diyala, Diyala 32001, Iraq

Corresponding author: Haidar N. Al-Anbagi (alanbagi@fel.zcu.cz)

ABSTRACT The popular small satellites already attracted attention towards the integration into the future ubiquitous Internet of Things (IoT) networks. Small satellites can act as IoT base stations to efficiently collect data from sensors in remote areas and offload it to ground stations (GSs). The size constraints of small satellites, however, impose limited power resources and tiny antennas onboard. Consequently, weak signals and outages are more probable at GSs. Therefore, GSs must utilize high gain antennas with complex and expensive steering resources to collect such weak signals through a single radio link. This traditional scheme can track only one satellite at a time with more vulnerability to outages resulting from possible severe signal degradations or from steering engine failures. To contribute to a successful integration of the popular small satellites into the future sixth generation (6G) inclusive IoT networks, this work validates the concept of diversity combining in improving the reception of small satellites signals. Six versions of the small satellite VZLUSAT-2's beacon were recorded by six simple software defined radio GSs registered at SatNOGS network and then combined. To assess the quality of the combined version, its errors are compared to the errors of the individual versions. According to the findings, if the GSs worked cooperatively in a diversity mode, they could generate a combined version that was always better than any other individually received stream. Furthermore, such a diversity-based scheme reduces the probability of outages and enables the simultaneous tracking of multiple satellites at each GS.

INDEX TERMS Cooperative reception, CubeSats, receive diversity, satellite Internet of Things, signals combining, SIoT, small satellites.

I. INTRODUCTION

The current terrestrial Internet of Things (IoT) networks maintain a variety of convenient services to countless users in urban and suburban areas. Examples of provided applications and services are smart transportation [1], [2], automated agile agriculture [3], intelligent traffic flow estimation [4], and smart healthcare monitoring [5], [6]. However, the present IoT coverage does not yet include less inhabited and harsh environments like deserts, oceans, forests, mountains, and poles [7]. Meanwhile, these uncovered areas are still fertile

The associate editor coordinating the review of this manuscript and approving it for publication was Adao Silva.

ground for many investigations, environmental observations, a home for many inhabitants, and a part of the whole universe in case of responding to natural disasters. This just emphasizes how crucial the aimed inclusive IoT coverage is in accommodating these harsh but rich environments. From the perspective of the service providers, it does not make practical nor economic sense to provide terrestrial infrastructures in these less inhabited areas. Therefore, the integration of satellites into terrestrial IoT networks became preferable for future ubiquitous IoT [7]. Attention has been paid towards small satellites in Low Earth Orbit (LEO) for further investigations in the evolving field of Satellite IoT (SIoT) [8]. The popularity of small satellites has surged recently due to their attractive

features of lower altitude, less delay, and lower predictable path loss [9]. To exploit such features, many experiments with IoT Long Range (LoRa) modulation format are already in operation for small satellites [10]. Small satellites are designed with light weight, compact size, and relatively fast manufacturing process providing cost-effective private space missions even to research groups and educational institutes. Concurrently, the development of ride-sharing launchers and reusable rockets has significantly reduced the cost to launch and deploy such satellites. Therefore, future sixth generation (6G) systems are seeking the aimed ubiquitous coverage through the integration of small satellites into the terrestrial IoT networks. The size restriction of such satellites, however, implies limited power and low gain antennas onboard. Thus, the receiving ground stations (GSs) experience higher levels of attenuations at the received signals with higher probability of communication outages. Therefore, the relevant GSs must deploy complex steering engines to precisely orient a high-gain directive antenna towards the satellite and establish a single radio link to collect such weak signals. This traditional single RF scheme is more prone to outages when having severe degradations or with steering engine failures. In addition, it allows the tracking of only one satellite at a time.

To contribute to a successful integration of the popular small satellites into the future IoT networks and to adopt a GS-based cheap solution, this study validates the concept of diversity combining in improving the reception quality of small satellites signals. The unprecedented solution utilizes one of the available simple and public software-defined radios (SDR) GSs networks with omnidirectional antennas to receive small satellite signals. These public GSs networks such as SatNOGS, SpyServer, Open-WebRx, and WebSDR do not yet work in a coordinated manner and do not perform any form of receive diversity combining.

Receiver-based diversity combining is a well-known technique which has been deeply studied, maturely developed, and widely applied in different mobile communication systems. For example, a site-based diversity was overviewed in [11] as an effective scheme to mitigate rain attenuation effects on satellites signals at tropical climates, a cluster diversity combining was suggested to accelerate the delivery of indoor autonomous vehicles' emergency alerts with less required rebroadcasts according to [12], a single-input multiple-output (SIMO) structure was presented to combine two downlinks from two receiving nodes by a Maximal Ratio Combiner (MRC) as a part of the study presented in [13] to improve the performance of a non-orthogonal multiple access (NOMA) network, the deep fading consequences inside tunnels were suppressed by utilizing multiple properly spaced antennas in a diversity scheme as confirmed in [14], MRC was deployed to enhance the performance by combining faded signals received by spatially distributed cellular base stations as depicted in [15], and the study conducted in [16] concluded

that increasing transmit and receive antennas improved the performance in high-mobility communication systems even when rapidly switching channels.

Enlightened by the surveyed literature, receive diversity has proven its effectiveness and reliability in improving the system performance in different applications. Nevertheless, receive diversity has not been previously investigated in satellite communications except in combining large and capable satellites' signals for improving the location accuracy as reported in [17], [18], and [19].

In earlier steps to this study, the authors investigated the concept of cooperative reception and combining on small satellites signals. In their investigative preliminary studies, the authors accomplished a simulation-based model in which N GSs were involved in a cooperative scheme to collect N versions of the same satellite downlink. The NGSs were supposed to be sufficiently apart to reflect different impairment levels at the N received versions. The N uncorrelated received versions were combined into one stream at different combining trials with a gradually increased number of the combined versions. The first trial was for a single site representing a non-diversity mode and the following trials were for combining 2, 3, 4..., and N versions, respectively. At each combining trial, the system performance was observed by calculating the number of errors (NOEs). To combine the records, a simple yet efficient technique was developed. At each combining trial, the combining algorithm constructs a square matrix by concatenating the streams involved in that trial on top of each other resulting in a matrix whose as many rows as the number of versions to combine. Then, at each column of the square matrix, the algorithm picks the most likely occurring value as the right value and stores it in the corresponding position of the combined stream. The proposed system model, the simulated cooperative reception, the developed post-detection combining algorithm, the system resources, and the concept of virtual ground station (VGS) were reported in [20] and [21]. The authors' third study, presented in [22], modified the algorithm to combine the received undetected symbols as a pre-detection combiner. The same study observed the system performance in engaging 12 sites under five scenarios: Uncorrelated SNRs of (0-11) dB, above average SNRs of (8-9) dB, correlated SNRs of (7) dBs, below average SNRs of (2-3) dB, and severe SNRs of 0 dBs except one site with 8 dB. Inspired by the model depicted in the simulation-based preliminary studies, demonstrated in Figure 1, this study is dedicated to validating the cooperative reception concept in combining multiple versions of a real small satellite signal. These versions are captured by real SDR GSs and shared with a VGS for combining.

To the best of the authors' knowledge, this is the first work to engage simple and public SDR GSs from open-source platforms like SatNOGS in a cooperative noncoherent manner to improve the reception of small satellites' signals, minimize the probability of communication outages, and offer to track several satellites at once.
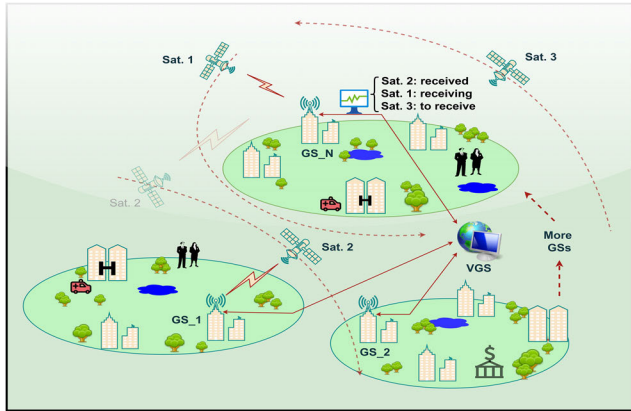
FIGURE 1. Cooperative reception of small satellites signals.

TABLE 1. Main features of VZLUSAT-2.

Aspect	Quantity
North American Aerospace Defense (NORAD) ID	51085
Initial altitude (km)	535
Downlink frequency (MHz)	437.325
Baud rate (beacon mode)	4800
Effective Isotropic Radiated Power (EIRP) (dBm)	~30
Date deployed	Jan. 26th 2022
Modulation format	MSK
Satellite documentation	[23]
Dashboard	[24]
Orbital observation	[25]

The rest of the article is organized as follows: Section II reveals the selected small satellite as a signal source, its orbital characteristics, and its transmission format. Section III presents the locations of the GSs to record the uncorrelated signals. Section IV exhibits the processing and the combining procedure. Section V presents the findings while Section VI concludes.

II. SIGNAL SOURCE

The small satellite, VZLUSAT-2, is selected as a signal source since the authors are currently part of the VZLUSAT-2's commanding team. VZLUSAT-2 is a Czech 3U nanosatellite of CubeSat type, where 1U is a cube of 10 cm a side. VZLUSAT-2's main mission is in-orbit demonstration and earth observation and has a main GS located at the University of West Bohemia in Pilsen, Czech Republic. The VZLUSAT-2's orbital speed is relatively high, indeed all small LEO satellites are, so that a one complete rotation around the earth takes approximately 95 minutes. Table 1 lists some of the features of VZLUSAT-2.

The high orbital speed results in a high Doppler effect and short communication window for the relevant GS. For such GSs, this adds another challenging factor to the limited transmitting power and low gain antennas of these small satellites. To convey the collected onboard data, VZLUSAT-2 utilizes the transmission mode (MSK AX.100 Mode 5) during the communication session to the main GS. According to the default setting of the transmission format, VZLUSAT-2 switches to the beacon mode 10-15 minutes after terminating the communication session with the main GS in Pilsen. In the beacon mode, VZLUSAT-2 sends a beacon signal every 10 seconds to indicate its healthy status to the operator and radio-amateur observers. In addition to healthy status, the beacon packet includes several fixed identifiers and synchronization signals such as periodic preamble for bit synchronization, sync-word for synchronization of packet beginning, header to indicate the type and length of useful data, and callsign of satellite. Therefore, recording multiple versions of VZLUSAT-2's beacon provides a great opportu-

nity for achieving the goals of this study in calculating the NOEs of the fixed part of the beacon packet in each individually received beacon as well as in the combined version.

The live orbital observation tool available at [25] was used to identify the locations of the ground terminals for recording the aimed multiple versions of the identifiers packet. On 11-03-2023, the time of recording the data in this study, VZLUSAT-2 was heading north towards the United States and Canada after passing over the main GS in Europe. Thus, possible VZLUSAT-2 visibilities to available GSs in these areas were further explored and scheduled.

III. SIGNAL RECORDINGS

As a reflection of the current popularity of amateur small satellites, many global platforms for networked SDR GSs have been recently developed. A great example is SatNOGS, where remote access for registered GSs' operators to calculate future passes of small satellites and schedule their observations is provided. In this study, SatNOGS was utilized to access the global network of GSs across Europe and United States, as shown respectively in Figures 2 and 3, and search for the visibilities of the VZLUSAT-2 after the time at which the communication to the main GS in Pilsen is terminated. Large number of observations are infeasible here because VZLUSAT 2 is a LEO satellite whose low altitude, high orbital speed, and high elevation angle needed for good communication. Furthermore, public open-source platforms like SatNOGS are still growing, and not yet widely spread.

The search revealed six observations as detailed in Table 2. For each recorded observation, SatNOGS provides a waterfall, an audio file of whole observation for further processing and analysis purposes, and decoded payload data (useful telemetry with fixed part of packet removed) in hexadecimal format only if the quality of the received signal is good enough for the built-in decoding tools. According to the cooperative reception model in Figure 1, the received audio signals must then be processed and combined in the VGS. As for processing the records, the time-discrete audio files are downloaded and used as described next.

IV. SIGNAL PROCESSING AND COMBINING

Once the recordings become downloadable to the dashboard of the observer, they must be offloaded into a PC in one
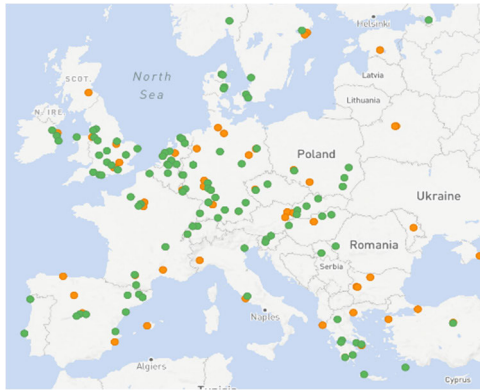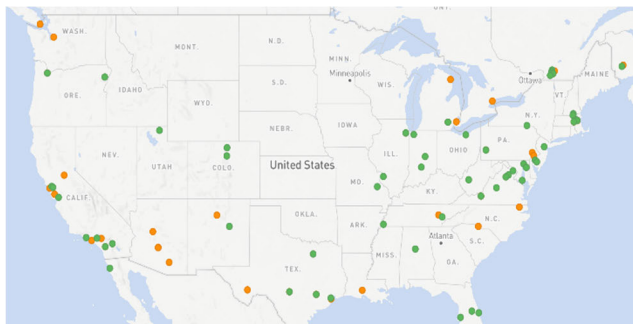
FIGURE 2. Registered SatNOGS GSs across europe.

FIGURE 3. Registered SatNOGS GSs across the US.

TABLE 2. Satnogs ground stations to record the signals.

No.	SatNOGS observation ID	Station name	Location	Time frame (HH:MM:SS)
1st	7260546	526-W2GRK	NJ, USA	02:22:51-02:28:01
2nd	7260550	2617-K2PI	VA, USA	02:23:05-02:27:07
3rd	7260625	385-52 HancockSt	MA, USA	02:24:06-02:27:27
4th	7260626	432-kc1fha	NH, USA	02:23:50-02:27:56
5th	7260638	1461-VE2DSK	QC, CA	02:22:07-02:31:17
6th	7260643	2834-kc0iyt	MA, USA	02:23:17-02:28:15

TABLE 3. Main features of utilized PC.

Aspect	Quantity
Operating system	Windows 10 Pro
Processor	Intel(R) Core(TM) i7-1065G7 CPU
Frequency	1.5 GHz
RAM	16 GB
System type	64-bit O.S., x64-based processor

directory for further processing and combining. The processing steps were performed in MATLAB using a PC whose features are listed in Table 3.
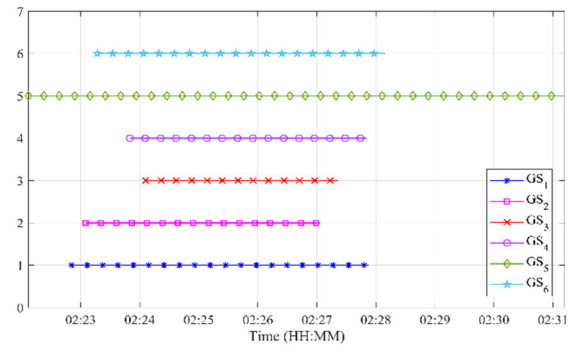

FIGURE 4. VZLUSAT-2's visibility times to the six GSs.

The following subsections clarify the developed algorithm's processing steps starting from initial visualizations of the collected recordings and ending at combining the VZLUSAT-2 identifiers packets.

A. PREPROCESSING: INITIAL VISUALIZATION
Before going into the analysis of the collected records, it is worth exploring when roughly each record starts and ends at, which records are the earliest and the latest, at what time the first overlapping occurs among the collected records' times, and accordingly when the combining becomes possible and when it is not. To explore such aspects, the algorithm loads the audio records into MATLAB and retrieves date, time, and length (in samples) of each record as a preprocessing step. Then, the algorithm sorts the times and identifies when the earliest and the latest visibilities of VZLUSAT-2 were, and to which GSs. To explore the overlapping of the records' times, they were visualized in a time manner in Figure 4, where the horizontal axis represents the observation time, and the vertical axis represents a shift for better visualization and has nothing to do with the power or the amplitude of the records.

According to the satellite's visibilities, the earliest observation was at (02:22:07) to the 5th GS while the latest one was at (02:31:11) to the 5th GS as well. The first overlapping in observations times was at (02:22:51) between the 5th and 1st observations whereas the last overlapping was at (02:28:09), the end of the 6th observation. In between the first and the last overlapping, signals combining was possible. The total visibility time for the six stations was (00:09:04) which corresponds to 544 seconds.

B. SEARCHING FOR IDENTIFIERS PACKETS
Communication systems always follow certain transmission formats with parts of known content that can help the receiver synchronize the received data packets. According to the VZLUSAT-2's documentation available at [23], the transmission mode switches to the beacon mode 10-15 minutes after the uplink/downlink session with the main GS terminates. When the beacon mode is active, VZLUSAT-2 regularly transmits a 64-bit preamble sequence followed by a 32-bit sync-word to indicate the start and end of the 24-bit header
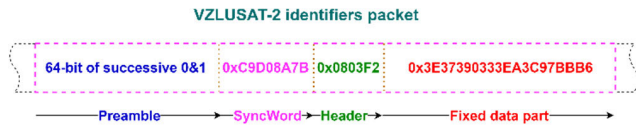
FIGURE 5. VZLUSAT-2 identifiers packet format and in a beacon mode.

and the 80-bit fixed part of the data stream, according to the documentation of VZLUSAT-2. The lengths and the contents of these patterns (i.e., satellite identifiers) are fixed by default in beacon mode. VZLUSAT-2's beacon is sent every 10 seconds to indicate the healthy status of the satellite. Therefore, searching for these patterns in the received signals and calculating their individual NOEs creates a great opportunity for this study to validate the diversity combining concept by comparing the individual NOEs to the combined version's NOE. The order and the default contents of the identifiers in the transmitted packet according to the documentation of VZLUSAT-2 are illustrated in Figure 5.

The identifiers' contents shown in Figure 5 in hexadecimal format are first converted into binary to result a 200-bit packet in its symbol-based format which is introduced in MATLAB to represent the default contents in their short format. Searching for the identifiers packet within the received audio records requires the conversion of the symbol-based packet into the long format where each symbol is represented by several samples according to the sampling and baud rates. The default sampling rate of the records from SatNOGS network is 48000 samples per second while the baud rate of VZLUSAT-2 is 4800 symbol per second which means every symbol is represented by 10 samples. Accordingly, the identifiers packet in its long format becomes 2000-sample long including the 640-sample preamble, 320-sample syncword, 240-sample header, and 800-sample for the fixed data part. Meantime, the received time-discrete audio records must also be converted to digital.

The algorithm then triggers the search process which tends to find a match for the 2000-sample packet or similar patterns in the received records considering a given error tolerance. After setting a tolerance of 400 errors for the 2000-bit identifiers packet, the algorithm searches for the best match of the identifiers packet in the received six records within a search window of four seconds to handle the slight asynchronized timeline of the recordings from the SatNOGS network due to latencies in the SDRs and computers used. The algorithm returns the start and end indices of the detected patterns and calculates NOEs present individually at each packet in the six records. Up to this step, the outcomes of the algorithm are the number of offloaded records, names of records' files, lengths of records (in samples), how many packets are detected in each record, start and end indices of each detected packet, and NOEs for each 200-symbol detected packet.

For the six records listed in Table 2, there were 14, 20, 9, 0, 38, and 10 found packets, respectively. Then, the algorithm checks for any redundant packets if spaced by less than the default spacing of 10 seconds and deletes them. Accordingly,

TABLE 4. Details of records and detected packets.

No.	SatNOGS observation ID	Lengths	Packets	Updated packets
1st	7260546	14490048	14	12
2nd	7260550	11425600	20	14
3rd	7260625	9407680	9	7
4th	7260626	11543104	0	0
5th	7260638	26155072	38	28
6th	7260643	14050624	10	7

TABLE 5. The required front and rear zeros for aligning the records.

No.	SatNOGS observation ID	Original lengths	Front zeros	Rear zeros
1st	7260546	14490048	2112000	9553024
2nd	7260550	11425600	2784000	11945472
3rd	7260625	9407680	5712000	11035392
4th	7260626	11543104	4944000	9667968
5th	7260638	26155072	0	0
6th	7260643	14050624	3360000	8744448

the algorithm modifies the number of detected packets and the corresponding information as depicted in Table 4.

Table 4 shows that the 4th record had communication outage and did not receive any detectable signal within the defined error tolerance of 400 errors. Therefore, the search for the identifiers' packets revealed no detected packets.

The next step is to align the records in a way so that the combining can be performed in a time manner with respect to the visibility of the satellite to the six GSs.

C. ALLIGNING THE RECORDS
Since the combining is intended to be in a time manner, the records must be aligned while maintaining their visibility order. To do so, the start and the end of each record are stretched and zero padded to match the start of the earliest and the end of the latest records, respectively. The zero padding extends the lengths of the records; however, it does not consume more resources in the processing because the identifiers' search process and identifying the start and end indices of each detected packet was done before the zero padding. Then, after performing the front and rear zero paddings for the purpose of aligning the records, the previously saved indices are only shifted by the number of the inserted zeros in the front padding process. The zero paddings of the six records are summarized in Table 5.

As shown in the Table 5, the 5th record neither did require zeros in the front nor in the rear paddings as it is the earliest and the latest observation. After the zero-padding process is complete, the start and end of the six records become aligned and have the same length of (26155072) samples.

D. COMBINING
After aligning the records, the next is to trigger the combining process. The combining algorithm checks in all records for

the availability of the identifiers packets whose start and end indices lie within the combining window of five seconds. Only if the algorithm finds multiple versions, they will be combined into one version. The combining window is shifted by three seconds at each combining trial regardless of whether the combining takes place or not until the window reaches the time of the latest record. At each combining trial, a counter is increased by one and the improvement of the system performance is observed by comparing the NOE of the combined version with the NOEs of all individual records. When it comes to the combining method, the authors developed their own simple yet efficient method. Before exploring the developed method, the known combiners in the literature should be briefly surveyed. Suppose at a combining trial, we have N versions (entrees) to combine. The algorithm concatenates the N identifiers' packets on top of each other to form a pre-combining matrix $\mathbf{C}$. The $\mathbf{C}$ matrix can be then represented as

$$C = \begin{bmatrix} pkt_1\,(1) & \cdots & pkt_1\,(end) \\ \vdots & \ddots & \vdots \\ pkt_N\,(1) & \cdots & pkt_N\,(end) \end{bmatrix}$$

where, pkt denotes the identifiers' packet.

According to selection combining (SC) method, the simplest known combiner in the literature, all versions must be evaluated and then the best version is selected [26], [27]. As a quality metric for evaluating the versions, signal to noise ratio (SNR) is usually utilized. Therefore, the combining according to SC can be expressed as selecting the nth packet with the lowest bit error rate (BER) as it corresponds to the highest SNR.

$$\min_{n \in (1:N)} BER\left(pkt_{n^{th}}\right) \quad (1)$$

However, this combining ignores the valuable information in the unselected *N-1* packets that might be beneficial in achieving higher improvement in the system performance. Moreover, SC leaves the improvement of combining N packets limited to only reach the quality of the selected version.

The most efficient but complex known combining method is maximal ratio combiner (MRC) [28]. After evaluating all entrees just like SC, MRC performs a weighting process by a set of adaptive weights. The adaptive weighting imposes more weight on the best version while weakening the worst one. Then, MRC combines the N weighted versions all together into one version whose quality is better than any other version among the entrees. However, the generated diversity gain when utilizing MRC comes on the price of system complexity as it requires evaluating N received streams, performing adaptive weightings, and then combining them into one. Accordingly, neither one of these known combiners met the goals of the presented study.

The main objective of this study is to propose a cheap ground-based solution to improve the reception quality of small satellites signals by applying a cooperative reception

scheme. Yet, the proposed solution must sustain an encouraging level of simplicity so that each single site gets motivated to join the diversity mode. Consequently, neither the simplicity of SC accompanied by limited improvement, nor the efficient but complex MRC is a good choice for the suggested cooperative reception scheme in this study. Indeed, a simple but efficient combiner is developed in this work to meet the aimed objectives. Rather than selecting only the best version as in (1), the developed combiner seeks for a combined packet (pkt_c) which is none of the received N packets. Therefore, the goal of the developed combining can be stated as in

$$\min_{c \notin (1:N)} BER\,(pkt_c) \quad (2)$$

Minimizing errors at the combined packet can also be interpreted in maximizing the likelihood of that combined packet to well approach the default content. Therefore, if given that all N packets are received, the likelihood of the combined packet (L_c) to maximize is:

$$L_c(pkt_c | pkt_1, pkt_2, \ldots, pkt_N) \quad (3)$$

Because the involved receiving sites are sufficiently apart, the received packets are independent and hence the likelihood in (3) becomes equivalent to the joint probability mass function (PMF) of the N packets,

$$\prod_{i=1}^{N} L_c(pkt_c | pkt_i) \quad (4)$$

Equation (4) expresses the likelihood quantity to maximize in the combining process for getting a combined stream that matches the default packet content the most. The goal expressed in (4) must be projected on the matrix $\mathbf{C}$ for combining N packets, i.e., N rows. To maximize the likelihood of the combined packet, the combiner relies on the most likely occurring bit of each column in $\mathbf{C}$ based on:

$$pkt_c\,(k) = \text{mode}\left\{pkt_1\,(k), pkt_2\,(k), \ldots, pkt_N\,(k)\right\} \quad (5)$$

where $k = 1, 2, \ldots,$ length (pkt_c) and mode (x) returns the most likely occurring value in the vector x.

Assuming the default packet is pkt_0, then we can express the probability of error (P_e) in the combined packet to be the probability (P_r) that the kth bit in the combined packet does not match the corresponding value at the position of pkt_0,

$$P_e\,(k) = P_r\left(pkt_c\,(k) \neq pkt_0\,(k)\right) \quad (6)$$

Minimizing the probability of errors (P_e) in the combined version corresponds to maximizing the probability (P) for getting a combined version pkt_c that can better match the original packet pkt_0. Thus

$$P\,(pkt_0 = pkt_c \mid pkt_{1:N}, H) \quad (7)$$

where H represents the matrix of the channels' impulse response. The probability in (7) can be also represented in

conditional probabilities according to [29],

$$P\left(pkt_0 = pkt_c \mid pkt_{1:N}, H\right) =$$
$$\frac{P\left(pkt_0 = pkt_c\right) f_{pkt_{1:N|pkt_0,H}}\left(pkt_{1:N} \mid pkt_0 = pkt_c, H\right)}{f_{pkt_{1:N|H}}\left(pkt_{1:N} \mid H\right)}$$
$$(8)$$

where the conditional probability terms at the denominator and numerator respectively represent the probability density functions (PDFs) of $pkt_{1:N}$ given H and $pkt_{1:N}$ given pkt_0 and H.

Because the term $P\left(pkt_0 = pkt_c\right)$ and the denominator PDF term are both independent of pkt_c, getting the probability (P) in the left side of (8) maximized corresponds to maximizing the only dependent PDF term:

$$f_{pkt_{1:N|pkt_0,H}}(pkt_{1:N}|pkt_0 = pkt_c, H)$$

Therefore, the maximum likelihood (ML) goal when combining $pkt_{1:N}$ to generate pkt_c can be expressed as

$$ML\left(pkt_c\right) = \underset{pkt_c \notin pkt_{1:N}}{\mathrm{argmax}}\, f_{pkt_{1:N|pkt_0,H}}\left(pkt_{1:N} \mid pkt_0 = pkt_c, H\right)$$
$$(9)$$

When reforming the PDF quantity in (9) using the standard multiple-input multiple-output (MIMO) communication systems [29] $pkt_{1:N} = Hpkt_0 + n_{1:N}$, we obtain

$$f_{pkt_{1:N|pkt_0,H}}\left(pkt_{1:N} \mid pkt_0 = pkt_c, H\right) = f_{n_{1:N}}\left(pkt_{1:N} - Hpkt_c\right)$$
$$(10)$$

where f_n represents the PDF of white Gaussian noise (n) according to [29]:

$$f_n\left(n\right) = \frac{1}{\left(\pi \sigma^2\right)^n} e^{-\frac{1}{\sigma^2}\|n\|^2}$$
$$(11)$$

Therefore, maximizing the left side of (10) is directly related to getting $\|n\|^2$ of pkt_c reduced. Indeed, the maximum likelihood of the combined stream can be met by minimizing the distance quantity $\left(pkt_{1:N} - Hpkt_c\right)$, or i.e.,

$$ML\left(pkt_c\right) = \underset{pkt_c \notin pkt_{1:N}}{\mathrm{argmin}} \|pkt_{1:N} - H\,pkt_c\|^2 \quad (12)$$

To reduce the distance term $\|pkt_{1:N} - Hpkt_c\|^2$, the developed combining follows the tendency of data at each column in **C**. The combining algorithm relies on the most likely occurring bit in each column to be the selected value at the corresponding position in the combined packet. This tendency-based combining should generate a combined packet whose less Euclidean distance to the original identifiers packet than any other individually received packet.

To validate the concept of the developed likelihood combining method, the combining process was applied on the aligned six records in this study. The combining algorithm navigates through the six records within a combining window of five seconds and checks for the possibility that more than two identifiers' packets are present. If it happens that
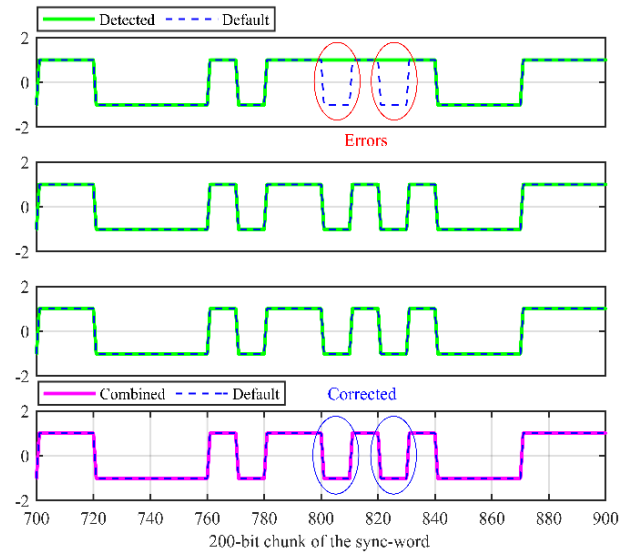

FIGURE 6. Combining 3 versions (200-bit long) of sync-word in trial 2.

a combining window includes more than two packets, the combining counter increases by one and the pre-combining matrix **C** is generated by concatenating the detected packets on top of each other. The next step is to convert the packets from the long sample-based format into the short symbol-based representation according to the ratio (sampling rate /baud rate) which yields 10 samples per symbol as mentioned in Section IV (B). Then, the likelihood combining is performed on each column in **C** to generate the combined version. For each combining trial, the algorithm computes the errors of the individual packets in addition to the error of the generated combined version.

V. RESULTS AND COMMENTS
From the time of the earliest observation to the time of the latest one, there were 11 combining trials and accordingly 11 combined packets were generated in this study. Because 11 trials of combining multiple 2000-bit versions of the identifiers packet are huge to visualize, only 4 trials of combining multiple 200-bit parts of the sync-word were selected and visualized. The 2nd, 3rd, 4th, and 5th combining trials are presented respectively in Figures 6, 7, 8, and 9. This collection of trials was carefully selected to provide sufficient insight into the combining method. Errors present in the individual versions are marked inside red ellipses. In the combined version, the corrected errors are marked inside blue ellipses while uncorrected ones are kept inside red ones.

Figures 6 and 7 show that errors present respectively in the first and second versions were corrected in the corresponding combined versions. In Figure 8, the combined version corrected errors only from the first version and uncorrected the ones from other versions because more than half of the entrees at these positions were errors. In the 5th combining trial, visualized in Figure 9, all errors from the second and fourth versions were corrected in the combined version.
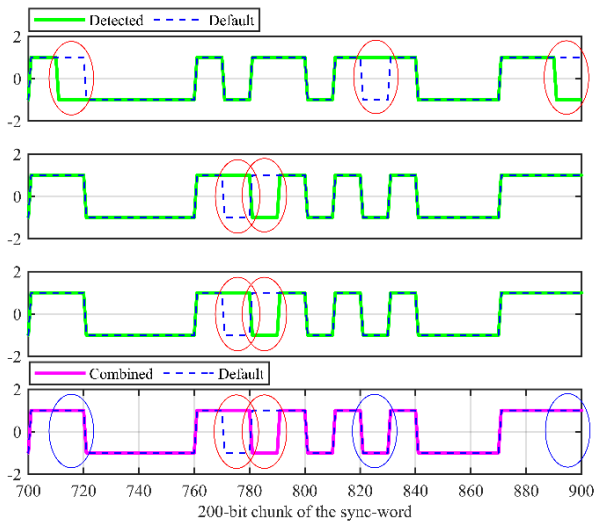
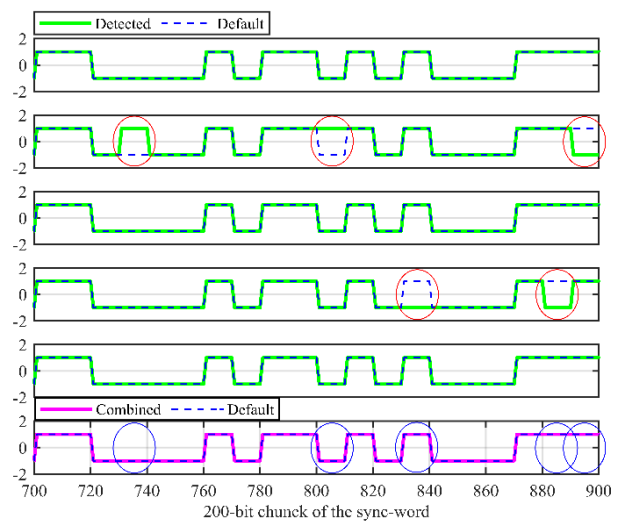**FIGURE 7.** Combining 3 versions (200-bit long) of sync-word in trial 3.

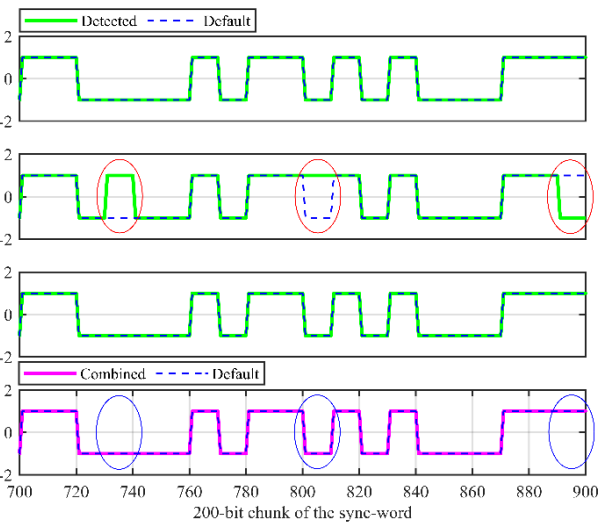**FIGURE 9.** Combining 5 versions (200-bit long) of sync-word in trial 5.

FIGURE 8. Combining 3 versions (200-bit long) of sync-word in trial 4.

FIGURE 10. Validating the combined version versus the 1ˢᵗ record.

In each presented trial, the combining of multiple versions corrected some errors and provided a better-quality version than some individual ones. However, that achieved quality was as good as some other individual versions. The question then becomes, does the proposed cooperative reception provide an improved performance to only some of the involved GSs? To find the answer, a more generalized assessment of the combined version is required. The quality of the combined packets must be compared to the quality of each individually received packet by the corresponding GS in a time manner. In the assessment, a referencing counter is set to zero and a time window of five seconds was generated to navigate through the generated combined packets with respect to the visibility time. Within each time window, the algorithm compares the NOE in the combined packet with the NOE of the packet available in each record individually. For instance, when validating the combined packets versus the packets in
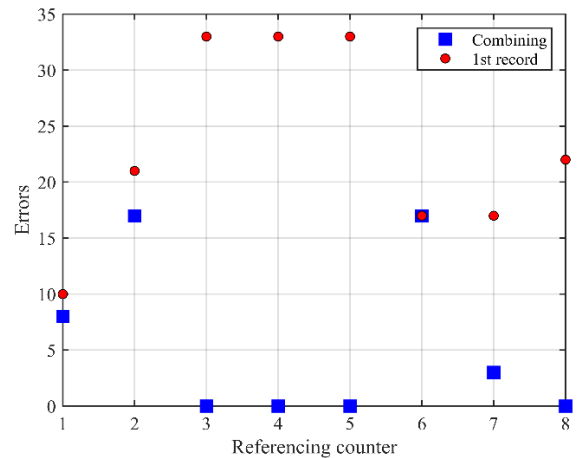
the first record, the referencing counter increases by one every time a combined packet is present along with a packet in the first record within the same window. Such a validation method provides a fair comparison for each GS and shows how beneficial or not to join the diversity-based reception scheme. Since the 4ᵗʰ GS experienced an outage and its record revealed no packets, the assessment process was performed versus the 1ˢᵗ, 2ⁿᵈ, 3ʳᵈ, 5ᵗʰ, and 6ᵗʰ records and the results are shown in Figures 10, 11, 12, 13, and 14, respectively. For more detailed validation results depicted in numbers, Tables 6, 7, 8, 9, and 10, are also provided accompanied with comments.

At all comparison points, the combining provided a better-quality packet than the corresponding packet in the 1ˢᵗ version. The accumulative NOE at the 1ˢᵗ records was 186 errors in 8 packets (corresponds to a BER of 0.11625), while the combined version brought it down to only 45 errors (corresponds to a BER of 0.028125) providing an improvement in the NOEs of 76 %.

TABLE 6. Comparing the combined version to the 1st record.

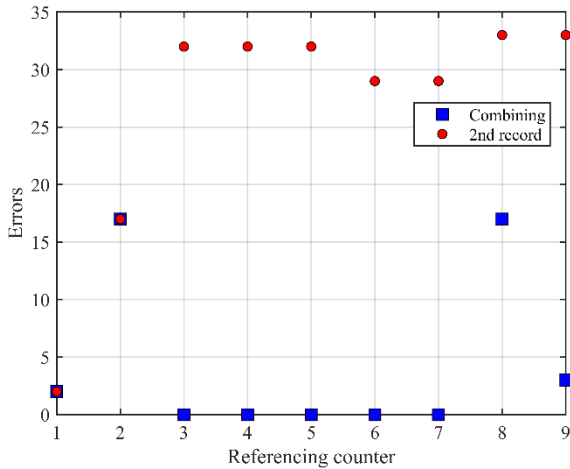| Referencing Counter	NOE @ 1st	NOE @ Combined	Improvement (%)
1	10	8	20
2	21	17	19
3	33	0	100
4	33	0	100
5	33	0	100
6	17	17	0
7	17	3	82
8	22	0	100

FIGURE 11. Validating the combined version versus the 2nd record.

TABLE 7. Comparing the combined version to the 2nd record.

Referencing Counter	NOE @ 2nd	NOE @ Combined	Improvement (%)
1	2	2	0
2	17	17	0
3	32	0	100
4	32	0	100
5	32	0	100
6	29	0	100
7	29	0	100
8	33	17	48
9	33	3	91

For the 9 packets in the 2nd record, the accumulative NOE was 239 errors (corresponds to a BER of 0.1327), while the NOE in the combined version was 39 errors (corresponds to a BER of 0.0216). Accordingly, the combining achieved an improvement of 84 % in the NOEs over the individually received data by the second GS.

The accumulative NOE at the 3rd records was 127 errors in 10 packets (corresponds to a BER of 0.064), while the combined version had only 30 errors (corresponds to a BER of 0.015) reflected an improvement in the NOEs of 77 % to the data received by the 3rd GS.

The accumulative NOE at the 5th records was 84 errors in 10 packets (corresponds to a BER of 0.042), while the NOE in the combined version was only 30 errors (corresponds to a BER of 0.015). As a result, the combined version provided an
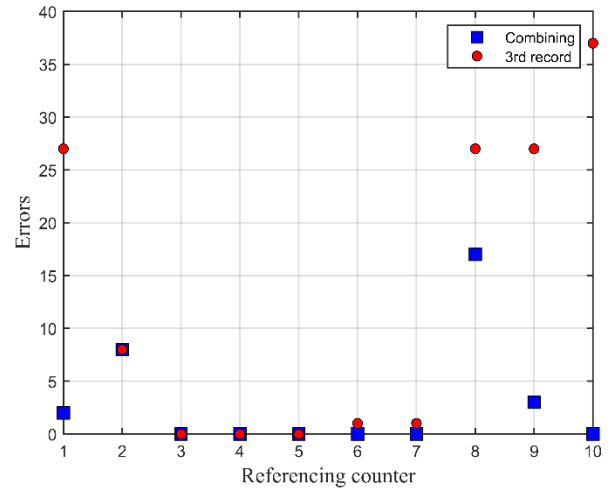

FIGURE 12. Validating the combined version versus the 3rd record.

TABLE 8. Comparing the combined version to the 3rd record.

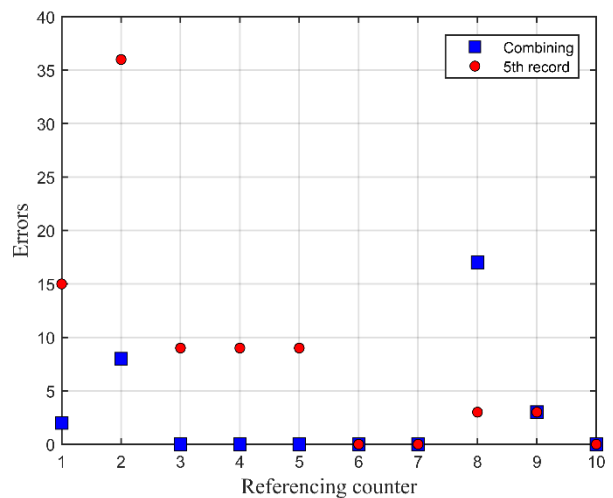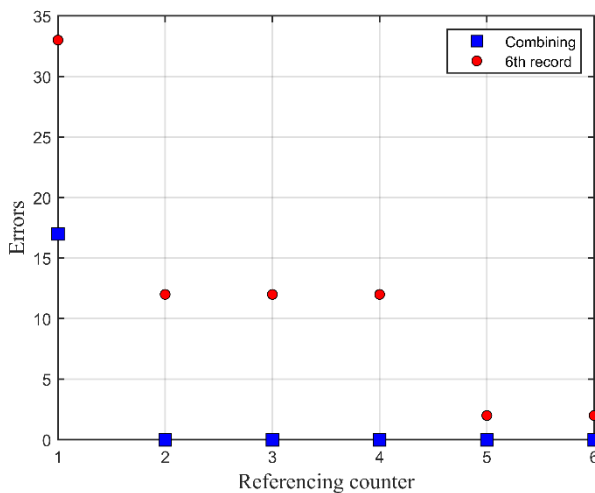| Referencing Counter	NOE @ 3rd	NOE @ Combined	Improvement (%)
1	27	2	93
2	8	8	0
3	0	0	0
4	0	0	0
5	0	0	0
6	1	0	100
7	1	0	100
8	27	17	37
9	27	3	89
10	37	0	100

FIGURE 13. Validating the combined version versus the 5th record.

improvement in the NOEs of 64 % compared to the packets received by the 5th GS.

The accumulative NOE at the 6th record was 73 errors in 6 packets which corresponds to a BER of 0.0608, while the combined version minimized it to only 17 errors which

TABLE 9. Comparing the combined version to the 5th record.

Referencing Counter	NOE @ 5th	NOE @ Combined	Improvement (%)
1	15	2	87
2	36	8	78
3	9	0	100
4	9	0	100
5	9	0	100
6	0	0	0
7	0	0	0
8	3	17	-82
9	3	3	0
10	0	0	0

FIGURE 14. Validating the combined version versus the 6th record.

TABLE 10. Comparing the combined version to the 6th record.

Comparison Counter	NOE @ 6th	NOE @ Combined	Improvement (%)
1	33	17	48
2	12	0	100
3	12	0	100
4	12	0	100
5	2	0	100
6	2	0	100

corresponds to a BER of 0.0141. Thus, the combined version provided an improvement of 77 % in the NOEs compared to the 6th version if received individually.

VI. CONCLUSION

Small satellites are very popular nowadays and have already attracted attention for the future integration in the 6G inclusive IoT networks. This study contributes to successful integration of such popular but limited resources satellites into the aimed future IoT coverage through a cooperative reception scheme (applied on the downlink direction where data are collected, stored, and retransmitted by the small satellites). In which, multiple GSs are networked to share

their individually received streams for further processing and combining. Inspired by simulation-based preliminary studies, this work tested the suggested reception scheme on combining 6 versions of real small satellite beacons collected by 6 GSs and turned out productive. When six versions of the nanosatellite VZLUSAT-2's beacon signal were separately recorded and then combined, the resulting version was always better than any other individual version. Indeed, for the six GSs in order, the improvements in the NOEs were 76%, 84%, 77%, 100%, 64%, and 77%. The validated reception scheme does not only minimize errors, but also reduces the probability that an involved GS experiences an outage. In fact, the 4th GS in this study had a communication outage and received no packets from the satellite. Nevertheless, under the cooperative scheme, this GS can be provided by a combined version whose quality is better than any other individual version from the remaining five stations. The generated diversity gain might be promising enough to even trigger the idea that such cooperative reception is capable of compensating the replacement of the present expensive steerable receiving antennas by affordable omnidirectional ones. Considering the doubled number of newly launched small satellites in only two years (2020-2022), the presented scheme precludes the need to build new expensive GSs for newly launched small satellite and proposes the utilization of current SDR based simple GSs as a huge network of cooperative nodes for non-coherent diversity combining of received signals. The diversity gain replaces the need for directional antennas on antenna rotators and the large frequency bandwidth of the signals digitized in SDR will allow such a network to cooperatively receive simultaneous simple data transmissions from a large number of small satellites.

REFERENCES

[1] N. Cao, Y. Chen, X. Gu, and W. Feng, "Joint bi-static radar and communications designs for intelligent transportation," *IEEE Trans. Veh. Technol.*, vol. 69, no. 11, pp. 13060–13071, Nov. 2020.

[2] N. Cao, Y. Chen, X. Gu, and W. Feng, "Joint radar-communication waveform designs using signals from multiplexed users," *IEEE Trans. Commun.*, vol. 68, no. 8, pp. 5216–5227, Aug. 2020.

[3] A. Salam and S. Shah, "Internet of Things in smart agriculture: Enabling technologies," in *Proc. IEEE 5th World Forum Internet Things (WF-IoT)*, Apr. 2019, pp. 692–695.

[4] A. H. A. Hussain, M. A. Taher, O. A. Mahmood, Y. I. Hammadi, R. Alkanhel, A. Muthanna, and A. Koucheryavy, "Urban traffic flow estimation system based on gated recurrent unit deep learning methodology for Internet of Vehicles," *IEEE Access*, vol. 11, pp. 58516–58531, 2023.

[5] T. Wu, F. Wu, C. Qiu, J.-M. Redouté, and M. R. Yuce, "A rigid-flex wearable health monitoring sensor patch for IoT-connected healthcare applications," *IEEE Internet Things J.*, vol. 7, no. 8, pp. 6932–6945, Aug. 2020.

[6] A. Hussain, K. Zafar, and A. R. Baig, "Fog-centric IoT based framework for healthcare monitoring, management and early warning system," *IEEE Access*, vol. 9, pp. 74168–74179, 2021.

[7] X. Fang, W. Feng, T. Wei, Y. Chen, N. Ge, and C.-X. Wang, "5G embraces satellites for 6G ubiquitous IoT: Basic models for integrated satellite terrestrial networks," *IEEE Internet Things J.*, vol. 8, no. 18, pp. 14399–14417, Sep. 2021.

[8] J. Chu, X. Chen, C. Zhong, and Z. Zhang, "Robust design for NOMA-based multibeam LEO satellite Internet of Things," *IEEE Internet Things J.*, vol. 8, no. 3, pp. 1959–1970, Feb. 2021.

[9] N. Saeed, A. Elzanaty, H. Almorad, H. Dahrouj, T. Y. Al-Naffouri, and M.-S. Alouini, "CubeSat communications: Recent advances and future challenges," *IEEE Commun. Surveys Tuts.*, vol. 22, no. 3, pp. 1839–1862, 3rd Quart., 2020.

[10] G. Álvarez, J. A. Fraire, K. A. Hassan, S. Céspedes, and D. Pesch, "Uplink transmission policies for LoRa-based direct-to-satellite IoT," *IEEE Access*, vol. 10, pp. 72687–72701, 2022.

[11] F. Samat, M. J. Singh, A. Sali, and N. Zainal, "A comprehensive review of the site diversity technique in tropical region: Evaluation of prediction models using site diversity gain of Greece and India," *IEEE Access*, vol. 9, pp. 105060–105071, 2021.

[12] S. Chang, "An emergence alert broadcast based on cluster diversity for autonomous vehicles in indoor environments," *IEEE Access*, vol. 8, pp. 84385–84395, 2020.

[13] D.-T. Do, T.-L. Nguyen, S. Ekin, Z. Kaleem, and M. Voznak, "Joint user grouping and decoding order in uplink/downlink MISO/SIMO-NOMA," *IEEE Access*, vol. 8, pp. 143632–143643, 2020.

[14] Z. Zhao, J. Wang, W. Hou, Y. Li, and B. Ai, "Optimized scheme of antenna diversity for radio wave coverage in tunnel environment," *IEEE Access*, vol. 8, pp. 127226–127233, 2020.

[15] A. Al-Rimawi, J. Siam, A. Abdo, and D. Dardari, "Performance analysis of dynamic downlink PPP cellular networks over generalized fading channels with MRC diversity," *IEEE Access*, vol. 9, pp. 39019–39027, 2021.

[16] X. Hou, J. Ling, and D. Wang, "Performance of high-mobility MIMO communications with Doppler diversity," *IEEE Access*, vol. 8, pp. 31574–31585, 2020.

[17] Z. Zhu, C. Jiang, and Y. Bo, "Performance enhancement of GNSS/MEMS-IMU tightly integration navigation system using multiple receivers," *IEEE Access*, vol. 8, pp. 52941–52949, 2020.

[18] P. Fan, X. Cui, and M. Lu, "Space and frequency diversity characterization of mobile GNSS receivers in multipath fading channels," *Tsinghua Sci. Technol.*, vol. 25, no. 2, pp. 294–301, Apr. 2020.

[19] E. Panholzer and S. Lindenmeier, "A new GNSS micro-diversity system," in *Proc. 52nd Eur. Microw. Conf. (EuMC)*, Sep. 2022, pp. 592–595.

[20] H. N. Al-Anbagi and I. Vertat, "Cooperative reception of multiple satellite downlinks," *Sensors*, vol. 22, no. 8, p. 2856, Apr. 2022.

[21] H. N. Al-Anbagi and I. Vertat, "Collaborative network of ground stations with a virtual platform to perform diversity combining," in *Proc. Int. Conf. Appl. Electron. (AE)*, Sep. 2022, pp. 1–6.

[22] H. N. Al-Anbagi and I. Vertat, "Pre-detection combining of small satellite downlink's replicas," in *Proc. Int. Conf. Electr., Comput. Energy Technol. (ICECET)*, Jul. 2022, pp. 1–6.

[23] VZLU. (Feb. 27, 2022). *The Main Systems of the VZLUSAT-2 Nanosatellite Put Into Operation*. [Online]. Available: https://www.vzlu.cz/the-main-systems-of-the-vzlusat-2-nanosatellite-put-into-operation/?lang=en

[24] SatNOGS. (Feb. 27, 2023). *VZLUSAT-2 Dashboard*. [Online]. Available: https://dashboard.satnogs.org/d/L8ywE9oMz/vzlusat-2?orgId=1&refresh=5s

[25] Cesium. (Feb. 27, 2023). *VZLUSAT-2 Live Orbital Observation*. [Online]. Available: https://pilsencube.zcu.cz/vzlusat2/over8.php

[26] M. K. Simon and M.-S. Alouini, "Digital communications over fading channels (M.K. Simon and M.S. alouini; 2005) [book review]," *IEEE Trans. Inf. Theory*, vol. 54, no. 7, pp. 3369–3370, Jul. 2008.

[27] H. Al-Hmood and H. S. Al-Raweshidy, "Selection combining scheme over non-identically distributed Fisher-Snedecor F fading channels," *IEEE Wireless Commun. Lett.*, vol. 10, no. 4, pp. 840–843, Apr. 2021.

[28] D. H. Tashman and W. Hamouda, "Physical-layer security on maximal ratio combining for SIMO cognitive radio networks over cascaded k-μ fading channels," *IEEE Trans. Cognit. Commun. Netw.*, vol. 7, no. 4, pp. 1244–1252, Dec. 2021.

[29] J. G. Proakis and M. Salehi, *Digital Communications*. New York, NY, USA: McGraw-Hill, 2001.

HAIDAR N. AL-ANBAGI (Member, IEEE) was born in Diyala, Iraq, in 1985. He received the bachelor's degree in communications engineering from the University of Diyala, Iraq, in 2006, and the master's degree in electrical engineering from the University of Bridgeport, Bridgeport, CT, USA, in 2013. He is currently pursuing the Ph.D. degree in electrical engineering with the University of West Bohemia, Pilsen, Czech Republic, under a Scholarship Program, between Czech Republic and Iraq.

He was nominated by the Higher Committee for Education and Development (HCED) with the Iraqi Prime Minister Office for a fully supported scholarship. His research interests include digital communications, signal processing, OFDM, MIMO systems, small satellites, cognitive radio, and the IoT applications.
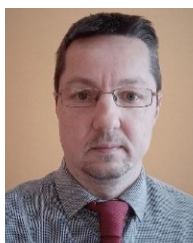
IVO VERTAT was born in Czech Republic, in 1980. He received the Ph.D. degree from the Faculty of Electrical Engineering, University of West Bohemia, in 2012. He is currently an expert in wireless communications and space hardware design. His Ph.D. thesis focused on developing efficient communication systems for picosatellites. Since 2009, he has been a member of the PilsenCUBE Team. Since 2017, he has operated the VZLUSAT-1. Since 2022, he has taken on the role of operating VZLUSAT-2 satellite. Additionally, he has been involved in exploring new concepts for ground stations that enable the operation of simple technological satellites without the use of antenna rotators. This novel approach eliminates the limitations of tracking only one satellite at a time, improving the efficiency of ground station operations.

• • •